Spectrochimica Acta Part A: Molecular and Biomolecular Spectroscopy 191 (2018) 277–282

Contents lists available at ScienceDirect

Spectrochimica Acta Part A: Molecular and Biomolecular Spectroscopy

journal homepage: www.elsevier.com/locate/saa

Photolysis study of octyl p-methoxycinnamate loaded microemulsion by molecular fluorescence and chemometric approach

Danielle Silva Nascimento, Matías Insausti, Beatriz Susana Fernández Band, Marcos Grünhut *

INQUISUR (UNS-CONICET), Department of Chemistry, Universidad Nacional del Sur, 1253, Alem Avenue, B8000CPB, Bahía Blanca, Argentina

ARTICLE INFO

Article history:
Received 29 May 2017
Received in revised form 5 October 2017
Accepted 9 October 2017
Available online 10 October 2017

Keywords:
O/W microemulsion
Octyl p-methoxycinnamate
Photolysis
Multivariate curve resolution-alternating least squares
Molecular fluorescence

ABSTRACT

Octyl p-methoxycinnamate (OMC) is one of the most widely used sunscreen agents. However, the efficiency of OMC as UV filter over time is affected due to the formation of the *cis*-isomer which presents a markedly lower extinction coefficient (ε_{cis} = 12,600 L mol^{-1} cm^{-1} at 291 nm) than the original *trans*-isomer (ε_{trans} = 24,000 L mol^{-1} cm^{-1} at 310 nm). In this work, a novel carrier for OMC based on an oil-in-water microemulsion is proposed in order to improve the photostability of this sunscreen. The formulation was composed of 29.2% (*w*/w) of a 3:1 mixture of ethanol (co-surfactant) and decaethylene glycol mono-dodecyl ether (surfactant), 1.5% (*w*/w) of oleic acid (oil phase) and 69.2% (w/w) of water. This microemulsion was prepared in a simple way, under moderate stirring at 25 °C and using acceptable, biocompatible and accessible materials for topical use. OMC was incorporated in the vehicle at a final concentration of 5.0% (*w*/w), taking into account the maximum permitted levels established by international norms. Then, a photolysis study of the loaded formulation was performed using a continuous flow system. The direct photolysis was monitored over time by molecular fluorescence. The recorded spectra data between 370 y 490 nm were analyzed by multivariate curve resolution-alternating least squares algorithm. The kinetic rate constants corresponding to the photolysis of the *trans*-OMC were calculated from the concentration profiles, resulting in 0.0049 s^{-1} for the *trans*-OMC loaded microemulsion and 0.0131 s^{-1} for the *trans*-OMC in aqueous media. These results demonstrate a higher photostability of the *trans*-OMC when loaded in the proposed vehicle with respect to the free *trans*-OMC in aqueous media.

1. Introduction

Currently, the search for more effective sunscreens to ensure optimal photoprotection is the latest research trend in this area. Sunscreen products are chemical absorbers (organic) or physical blockers (inorganic) that have the ability to filter out UVB rays (290–320 nm), because this type of rays are responsible for sunburns. Not only is there the high capacity of UV-filters to absorb UV, but there is also the property of remaining stable while irradiated [1,2]. The filter should not impair the absorbance for the entire period of sun exposure in order to achieve the expected photoprotection for commercial sunscreen products [3].

The octyl-p-methoxycinnamate (OMC) is one of the organic molecules widely used as sunscreen in topical preparations and ideal to use in waterproof products because of their lipophilicity. Their application is well tolerated and the skin irritation is almost negligible. OMC is used mainly as a UVB filter although its absorption spectrum extends into the UVA (320 nm–400 nm) [4]. However, this UV filter has shown to be light sensitive with a decrease in UV absorption efficiency upon light exposure [5]. For this reason, suitable vehicles have been designed as carriers for OMC in order to enhance their photostability. Thus, polymeric nanocapsules [6], lipid nanoparticles [7] and solid lipid nanoparticles [8] have been utilized as potential vehicles for OMC sunscreens.

Microemulsions (MEs) are transparent and thermodynamically stable systems that have a droplet size from 10 to 200 nm and do not have a tendency to coalesce [9]. MEs present advantages such as allowing the release of the substance encapsulated in a sustained manner and the ability to protect labile compounds against chemical degradation and photodegradation induced by UV radiation [10]. Moreover, all the typical components of the MEs such as oil, water, cosurfactants and surfactants are usually good permeation enhancers. All these characteristics of the MEs showed a significant enhancement effect on transdermal delivery over the conventional formulations.

On the other hand, kinetic rate constants are useful because they allow to predict chemical behaviour under yet unexplored conditions and to compare different chemical systems. Particularly, the spectroscopic monitoring allows the obtainment of large amounts of data corresponding to a reaction, in short periods of time. Multivariate methods as multivariate curve resolution-alternating least squares (MCR-ALS) explore the advantage of using a very high number of analytical signals simultaneously. This algorithm allows to extract the

* Corresponding author.
E-mail address: mgrunhut@uns.edu.ar (M. Grünhut).

https://doi.org/10.1016/j.saa.2017.10.025
1386-1425/

pure spectra and concentration of the components in a mixture from a set of spectra with a different composition [11,12]. This feature is particularly useful to evaluate the kinetic profiles of the chemical process [13]. Traditionally, kinetic studies require aliquots to be analyzed externally. When multivariate methods are applied, the spectroscopic data can be modelled using hard or soft models. The hard-modelling methods require a reaction of the model to be assumed and the goal is to extract the basic parameters of the process. The correct choice, when in-depth chemical knowledge of the system is not available, depends on tedious trial-and-error procedures. Furthermore, the mathematical soft-modelling methods are used in the cases that an explicit kinetic model cannot be postulated. Besides, the residual signals from species that do not take part in the reaction can be modelled.

The hybrid soft and hard-modelling incorporates constraints to force some or all the concentration profiles to fulfill a kinetic model, which is refined at each iterative cycle of the optimization process [14]. Thus, soft modelling is measure-driven, being able to resolve only the contributions with an explicit signal. However, the inclusion of a hard-modelling constraint will allow the introduction of a signal that comes from species without a registered signal.

The current article proposes a new O/W microemulsion as a carrier for OMC. The system was properly characterized and a photolysis study was performed using a continuous flow system which was monitored by molecular fluorescence spectroscopy. The spectral data as a function of time were analyzed by MCR-ALS algorithm. The use of this chemometric approach made it possible to study the photolysis kinetic behaviour of the OMC without using separation techniques. Moreover, the kinetic rate constants associated to the photoisomerization of the OMC were obtained as additional information. Finally, the solar protector factor was obtained in order to determine the efficiency of the OMC loaded ME as sunscreen.

2. Experimental

2.1. Reagents

All the reagents were analytical-grade chemicals and ultra-pure water (18 MΩ cm^{-1}) was used. Decaethylene glycol mono-dodecyl ether (DME; Sigma-Aldrich) and ethyl alcohol (ET; Dorwil) were used as non-ionic surfactant and co-surfactant, respectively. Oleic acid (OA; Applichem) was used as oil phase and octyl-p-methoxy cinnamate (OMC; Parafarm) was used as UVB filter.

2.2. Methods

2.2.1. Pseudo-Ternary Phase Diagram

The pseudo-ternary phase diagram was performed using the aqueous titration method at room temperature (25 °C). The weight ratio of surfactant (DME) to the co-surfactant (ET) was 3:1. In each system, the mixture of DME:ET (3:1) was mixed with the oil (OA) at weight ratios ranging from 9:1 to 1:9 (% *w*/w). Each weight ratio mixture was then gradually titrated with ultra-pure water, under moderate magnetic stirring. According to the ratio components of the mixture (oil phase, water and surfactant), different structures and a number of phases could be reached. These different structures could be seen by their physical appearance. Taking into account that microemulsions can be defined as transparent systems, the mixtures were visually examined in terms of transparency.

2.2.2. Characterization of MEs

The average droplet size, polydispersity index (PI) and conductivity measurements were determined by dynamic light scattering (DLS) using a Malvern Zetasizer Nano Series instrument. The measurements were performed at room temperature and at a 90° angle.

The morphology of the O/W MEs was evaluated by transmission electronic microscopy (TEM). A drop of the O/W ME was transferred onto a Formvar coated copper grid (200 mesh), followed by negative staining with uranyl acetate solution for 1 min. The sample was dried at room temperature and the TEM was performed using a JEOL 100 CXII transmission electron microscope, operated at 80 kV.

2.2.3. Preparation of OMC Loaded MEs

OMC was added to the ME in order to obtain a final concentration of 2.5, 5.0 and 7.5% (*w*/w). These dosages were chosen taking into account the technical specifications for the United States Food and Drugs Administration and the European Union, which authorize a maximum level of 7,5 and 10% (*w*/w), respectively [15]. OMC was added to the oil phase by stirring at 25 °C. Hence, this mixture was added to the DME:ET (3:1) mixture and titrated with ultra-pure water under moderate magnetic stirring. All prepared OMC loaded MEs were stored in amber-glass containers at room temperature (25 °C).

2.2.4. Photolysis Study

The photolysis study of the OMC was performed using a continuous flow system in both, aqueous medium (OMC-AQ) and loaded in the O/W microemulsion (OMC-ME). The OMC-AQ was prepared in order to obtain a final concentration of 5.0% (*w*/w). At first, due to the fact that OMC is a lipophilic molecule, it was diluted in ethanol. Then, water was added until the final concentration. The OMC-AQ and OMC-ME were pumped with a Watson 323 peristaltic pump. All the flow system components were made of PTFE (0.5 mm i.d.). A lab-made photoreactor was constructed, rolling helically PTFE (12 m in length) around a Philips® low mercury UVB lamp (15 W). The fluorescence measurements were performed using a Jasco FP-6500 spectrofluorometer. The slit width was 3 nm for excitation and 3 nm for emission. The excitation wavelength was 354 nm and the emission spectra were recorded between 370 and 550 nm. The scan rate was 500 nm min^{-1}. The acquisition interval and integration time were maintained at 0.1 nm and 1.0 s, respectively. The photomultiplier tube (PMT) voltage was fixed to 600 V and a flow quartz cell with 150 μL was used in a right-angle geometry.

The OMC-AQ and OMC-ME were pumped to the photoreactor and when it was filled, the UVB lamp was turned ON for 12 min. The flow rate was optimized in order to elute the loaded volume in the photoreactor (9.42 mL) in 12 min. Fluorescence spectra were registered every 30 s, adding 24 spectra per sample. The emission signals were registered every 0.1 nm, so each spectrum consisted of 1800 variables. Therefore, each sample was arranged in a matrix of 24×1800 variables. The data analysis was performed by MCR-ALS using MCR-ALS_GUI_2.0 toolbox [16] written in MatLab® environment [17]. This algorithm consists of a mathematically decomposition of the analytical signal into the contributions due to the pure components in the system, which can be written as a bilinear model of pure component contributions, as follows:

$$\mathbf{D}=\mathbf{C}\mathbf{S}^{\boldsymbol{T}}+\mathbf{E} \quad (1)$$

where **D** is the experimental fluorescent data matrix, **C** is the matrix describing the changes in the concentration of the species present in the system under study, $\mathbf{S}^T$ is the matrix containing the fluorescent spectra of these species, and **E** is the residual matrix with the data variance unexplained by $\mathbf{CS}^T$. The modelling started by selecting the number of components that caused the variations in the fluorescent spectra (chemical rank). The second step was the estimation of the pure spectra corresponding to the chemical components ($\mathbf{S}^T$). Then, an iterative optimization was done and the concentrations of the species (**C**) were calculated using the initial spectra estimations. Hence, using the fluorescent data and the concentrations, the pure spectra was re-estimated; **C** and $\mathbf{S}^T$ were repeatedly calculated until achieving an establish difference among iterations. During the optimization, some constraints were applied, such as, non-negativity for both, spectra and concentration profiles. On the other side, a constraint related to the proposed kinetic model (pseudo-first order) was considered. Moreover, it required some initial information: the starting concentrations for each

species, which was considered in the model, a vector specifying the times of the reaction and an initial estimate of the kinetic rate constants.

2.2.5. Solar Protection Factor (SPF) Determination

The SPF for the 5.0% (*w*/w) OMC-ME was obtained *in vitro* by Mansur method [18]. For this, the ME was diluted in ethanol at a final concentration of 0.2 mL mL^{-1}. The spectrophotometric measurements between 290 and 320 nm and each 5 nm were performed using a Hewllet Packard 8453 UV–Vis spectrophotometer equipped with a quartz cell (10 mm optical path). The SPF was calculated as detailed below:

$$SPF = CF \sum_{290}^{320} EE_{(\lambda)} \; I_{(\lambda)} \; A_{(\lambda)} \quad (2)$$

where *CF* is a correction factor (in this case, 10), EE is the erythemal effect spectrum, I is the solar intensity spectrum and A is the measured absorbance of the OMC-ME at each wavelength. The relationship between the erythemal effect spectrum and the solar intensity spectrum at each wavelength (EE x I) was determined as described by Sayre et al. [19].

3. Results and Discussion

3.1. Pseudo-Ternary Phase Diagrams

The pseudo-ternary phase diagrams were performed to find out the concentration range of components easily in order to create microemulsions. The studied systems were composed of the whole constituents including DME, ET, OA and water. A 3:1 surfactant and co-surfactant ratio (DME:ET) exhibited the largest ME domain and stability, among the other systems tested whose DME:ET ratios were 1:1 and 2:1. Therefore, the 3:1 ratio was used in this work and it was named Smix. The corresponding pseudo-ternary phase diagram is shown in Fig. 1.

3.2. Characterization of MEs

Based on the O/W microemulsion region corresponding to the pseudo-ternary phase diagram, six O/W microemulsions were prepared at different component ratios as described in Table 1.

Mean droplet size and polydispersity index (PDI) are important parameters in designing novel carriers based on MEs. PDI represents the ratio of standard deviation to mean droplet size. A PDI between 0.2 and 0.4 indicates a narrow size distribution of the globule size approaching a monodisperse system (for an ideal uniform sample, the PDI would be zero). Table 2 shows these parameters obtained by the

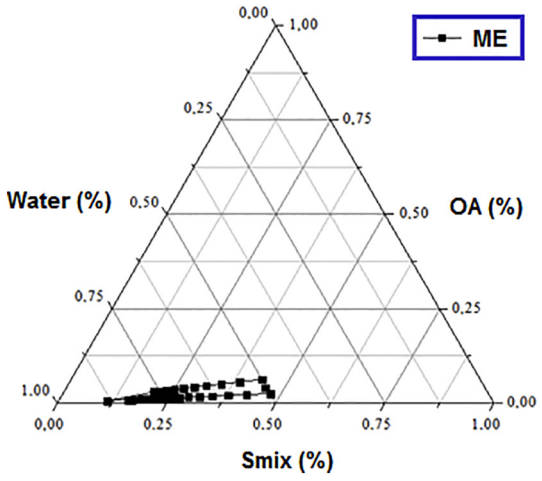

Fig. 1. Pseudo-ternary phase diagram corresponding to the oil-surfactant:co-surfactant-water system at 25 °C. Smix correspond to a 3:1 weight ratio of DME:ET.

Table 1
Composition of studied O/W microemulsions.

Formulation	Composition (% w/w)		
	OA	Smix	Water
ME1	2.0	38.0	60.0
ME2	1.8	34.5	63.6
ME3	1.7	31.7	66.7
ME4	1.5	29.2	69.2
ME5	1.4	27.1	71.4
ME6	1.3	25.3	73.3

DLS technique, corresponding to the six MEs analyzed. As can be seen, the MEs presented droplet sizes in the range from 11 to 14 nm and PDI values lower than 0.36. These values showed the uniformity of the drops within the formulations, indicating stable and monodisperse systems. Furthermore, small Z potential values were expected to confer a high physical stability to the MEs with a low tendency to flocculate globules. The droplets exhibited a slightly negative Z potential values, indicating a negative surface which would inhibit their aggregation (Table 2). These results are probably due to the use of non-ionic surfactants. Besides, the microemulsions presented relatively high conductivity values, indicating O/W microemulsions (Table 2).

Moreover, the droplet size of the six microemulsions was measured during 30 days (Fig. 2). The droplet size slightly increases as the OA and Smix concentration is lower, within the studied ranges (Table 1). However, in all cases, the droplet sizes were less than 20 nm and these were stable during 30 days.

Based on the results obtained by the DLS technique, the stability of the parameters over time, and taking into account the relatively low concentrations of OA and Smix used, the ME4 was considered for further studios. A relatively short time (about 5–10 min) was required to obtain ME4 under magnetic stirring at 25 °C, which is composed of 1,5% of OA, 29,2% of Smix (3:1) and 69.2% of water. In order to corroborate the droplet size and analyze the morphology of the droplets in the ME4, a TEM study was performed and the photos are shown in Fig. 3.

As seen, ME4 presented a spherical morphology and droplet sizes in nanometric range according to the results obtained by the DLS technique.

Hence, OMC was loaded in ME4, as described in section 2.2.3. The OMC-MEs were characterized by the DLS technique. The physic and physicochemical parameters were similar to non-loaded OMC O/W microemulsion when a 5.0% (*w*/w) of OMC was loaded (droplet size: 13.67 nm; PDI: 0.285; Z potential: −0.690 mV; conductivity: 0.131 mS cm^{-1}). Therefore, the incorporation of 5.0% (w/w) of OMC to ME4 did not affect the properties of this carrier significantly, and further studies were performed.

3.3. Photolysis Study

A photolysis study was performed in order to compare the photolysis process of the OMC when it is presented in an aqueous medium (OMC-AQ) with respect to the OMC loaded in the O/W microemulsion (OMC-ME). For this purpose, the continuous flow system described in section 2.2.4 was used.

Table 2
Physicochemical parameters of the O/W microemulsions.

Formulation	Droplet size (nm)	PI	Zeta Potential (mV)	Conductivity (mS cm^{-1})
ME1	11.56	0.312	−0.429	0.122
ME2	12.45	0.361	−0.496	0.129
ME3	13.56	0.307	−0.664	0.128
ME4	13.98	0.278	−0.762	0.127
ME5	12.76	0.280	−0.859	0.117
ME6	14.23	0.308	−0.888	0.121

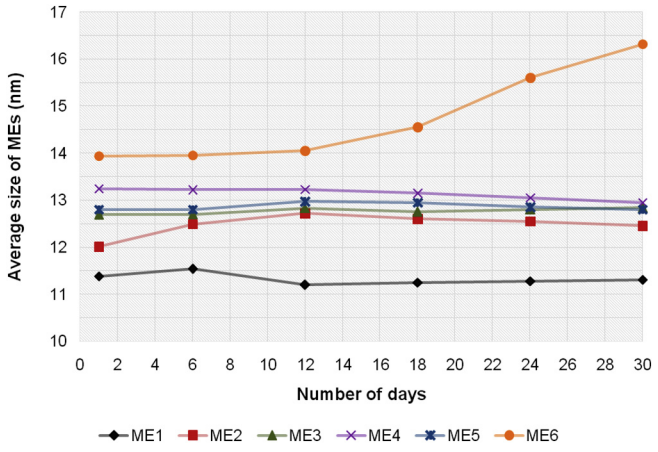

Fig. 2. Droplet size along 30 days for the six O/W microemulsions analyzed.

The direct photolysis of the OMC in an aqueous medium produces their photoisomerization, which octyl p-methoxy-trans-cinnamate (*trans*-OMC) changes to octyl p-methoxy-cis-cinnamate (*cis*-OMC), as follows:

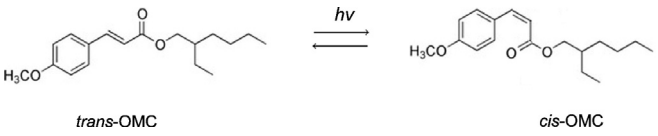

trans-OMC *cis*-OMC

The *trans*-isomer has an absorption wavelength similar to the *cis*-isomer (291 nm for the *trans*-isomer and 310 nm for the *cis*-isomer) but the molar absorption coefficient of the *cis*-isomer (ε_{cis} = 12,600 L mol^{-1} cm^{-1}) is markedly lower than *trans*-isomer (ε_{trans} = 24,000 L mol^{-1} cm^{-1}), at the respective wavelengths. This fact results in a reduction of the OMC efficiency as UV filter [20]. It is important to note that the decrease in the absorptivity occurs in both, aqueous and microemulsion medium. Moreover, the photolysis of OMC is followed by a photodegradation and photodimerization process, where several by-products are generated, such as, 4-methoxybenzaldehhyde, 2-ethylhexanol, cyclodimers and a dimer hydrolysis product [5].

On the other hand, the photoisomerization process can be monitored by molecular fluorescence because *trans*-OMC and *cis*-OMC are fluorescent molecules. Both presented maximum excitation wavelengths at 354 nm. However, the maximum emission wavelengths for the *trans*-OMC and the *cis*-OMC were 410 and 405 nm, respectively, demonstrating a shift of the maximum emission wavelength for *trans*-OMC during the photoisomerization process (Fig. 4).

In this way, fluorescence spectra corresponding to OMC-AQ and OMC-ME were registered as a function of irradiation time. A maximum time of 12 min was considered because after that the fluorescent signal was approximately constant. This means that the UVB radiation did not photodegradate substantially more filter, under the studied conditions. Besides, the spectral behaviour of the aqueous and microemulsion media were evaluated (Fig. 4).

As may be seen, the spectra corresponding to OMC-AQ and OMC-ME (Fig. 4 c and d, respectively) showed a decrease in the fluorescence signal intensity between 370 y 490 nm over time. In the case of OMC-AQ, the few spectra registered until reaching the degraded state showed that the photoisomerization of *trans*-OMC to *cis*-OMC occurs in a short time. Instead, the OMC-ME showed more spectra registered, which means that the photolysis leads takes longer. Furthermore, fluorescence spectra of the media (aqueous and microemulsion) were registered (Fig. 4 a and b) and small differences can be observed over irradiation time. Thus, the decrease in the fluorescence signal in OMC-AQ and OMC-ME is mainly due to the OMC photoisomerization process, in both cases.

The collected photolysis data contain information about the species involved in the process. Hence, the spectral data were arranged in matrices, which were disaggregated using the MCR-ALS algorithm. As mentioned before, this decomposition concluded in the pure spectra of the constituents of the samples, and most importantly to the kinetic study about the evolution profiles of the species in function of irradiation time. The acquired spectra profiles corresponding to the photolysis of OMC-AQ and OMC-ME are shown in Fig. 5.

As seen, the concentration profile of a third component was presented. Then, the reaction mechanism that best fitted was considering this fact, as follows: A → B and B → C. This approach is in concordance with the one mentioned before, as the photoisomerization of OMC is followed by a photodegradation and photodimerization process, where some by-products are generated [5,21].

The constraints that were incorporated in the MCR-ALS optimization process, can partially model the evolution of some components by means of a hard-modelling. This is performed by fitting the spectroscopic data to a model built from mathematical expressions. For the rest of the components of the system it was appropriate to use a soft-modelling. For this reason, a hybrid soft and hard-modelling was performed because the photolysis of OMC takes place among other registered signals coming from the medium. Afterwards, the concentration and spectral profiles can be obtained even though the compounds or interferences do not take part in the explicit model.

In that way, the kinetic rate constants of OMC-AQ and OMC-ME were calculated using the profiles shown in Fig. 5 (blue lines). As seen, the curves showed a reduction in the photoisomerization rate over time in both, OMC-AQ and OMC-ME. The decrease of OMC concentration over time followed a pseudo-first order kinetic:

$$\ln\left[(C_t - C_{inf})/(C_0 - C_{inf})\right] = k\,t \quad (3)$$

where C_t is the concentration of OMC at time t, *Cinf* is the concentration

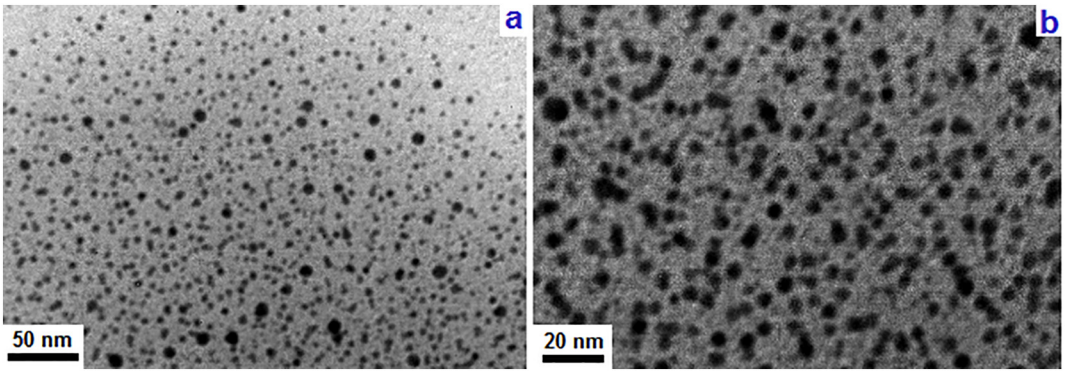

Fig. 3. TEM images of the ME4, with a magnification of 140,000× (a) and 270,000× (b).

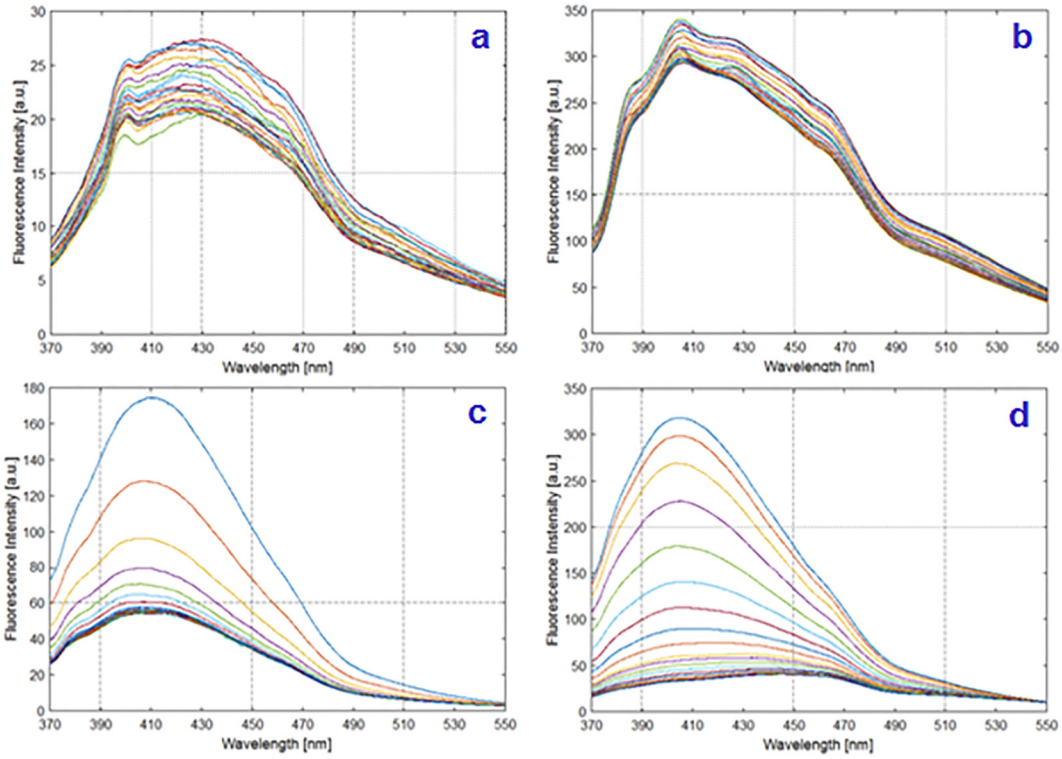

Fig. 4. Fluorescence spectra as a function of irradiation time (recorded every 30 s): a) aqueous medium, b) O/W microemulsion, c) OMC-AQ and d) OMC-ME.

at infinite time, C_0 is the initial concentration of OMC, t is the photoisomerization time in seconds and k is the kinetic rate constant. Fig. 6 shows the linear fit curves corresponding to the pseudo-first order kinetic photoisomerization of OMC in both, aqueous medium (OMC-AQ) and in the proposed microemulsion (OMC-ME). The calculated kinetic rate constants k were 0.0131 s^{-1} and 0.0049 s^{-1} for OMC-AQ and OMC-ME, respectively. These values showed a higher photoisomerization rate for OMC-AQ than for OMC-ME, indicating that the microemulsion protects OMC from the photoisomerization induced by the UVB radiation, under the studied conditions. Both models were well explained with 99.38% and 99.97% of explained variance, respectively.

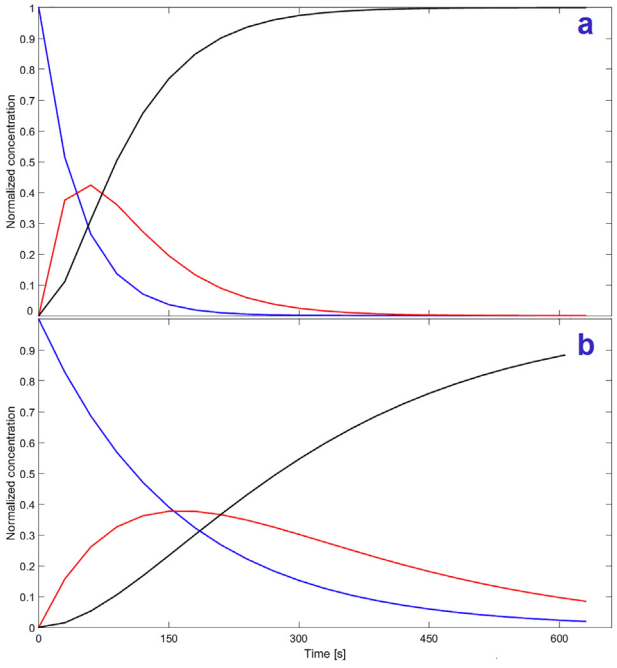

Fig. 5. Pure concentration profiles corresponding to the photolysis of OMC: a) in aqueous medium (OMC-AQ) and b) loaded in the proposed O/W microemulsion (OMC-ME). The blue lines correspond to *cis*-OMC, black lines to *trans*-OMC and red lines to a by-product. (For interpretation of the references to colour in this figure legend, the reader is referred to the web version of this article.)

3.4. Solar Protection Factor Determination

In order to know the efficacy of the proposed OMC-ME as sunscreen, the determination of the SPF was performed, which is a very useful reference when choosing a commercial sunscreen. The SPF can be defined as the relation between the UV energy required to produce a minimal erythema dose (MED) on protected skin and the UV energy required

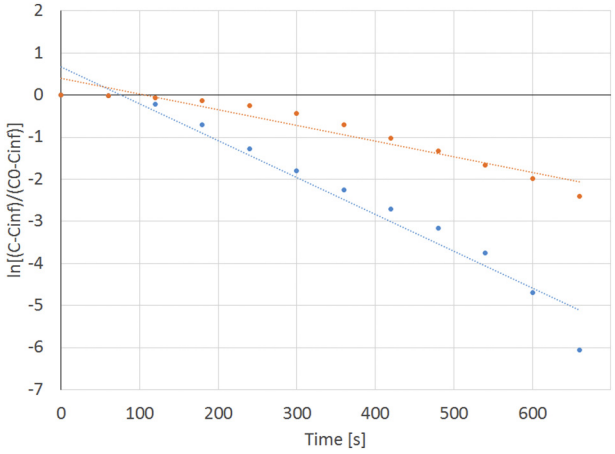

Fig. 6. Linear fit curves corresponding to the pseudo-first order kinetic photodegradation of OMC-AQ (red) and OMC-ME (blue). (For interpretation of the references to colour in this figure legend, the reader is referred to the web version of this article.)

to produce a MED on unprotected skin, and calculated as:

$$SPF = \frac{\text{MED in sunscreen} - \text{protected skin}}{\text{MED in nonsunscreen} - \text{protected skin}} \quad (4)$$

MED is the lowest time interval or dosage of UV radiation sufficient to produce a minimal and perceptible erythema on unprotected skin [22]. When higher the SPF is, more effective the sunscreen is in preventing sunburns. An *in vitro* method to obtain the SPF is proposed by Mansur et al. [18] (and described in section 2.2.5) in which the absorption of the sunscreen is based on the spectrophotometric analysis of dilute solutions. This method presents an optimal correlation with *in vivo* studios for SPF determination [23]. Then, the SPF value obtained (in triplicate) by Mansur et al. method for the proposed OMC-ME was 7.75. This result can be considered optimal, taking into account that the studied formulation was loaded with an unique sunscreen, and it was in concordance with previous works where OMC was present in a similar concentration (5,0%), as used in this studio [24].

4. Conclusions

The study demonstrated that the proposed O/W microemulsion could be an effective carrier for OMC. The proposed system was physicochemical characterized and its morphology analyzed, demonstrating a stable O/W microemulsion over time. Based on the kinetic rate constants obtained by the photolysis study assisted by MLR-ALS algorithm, we can conclude that the OMC photoisomerization was slower when it was present in the O/W microemulsion, in comparison to the OMC in an aqueous medium. Therefore, the proposed O/W microemulsion could be an appropriate carrier for OMC because it improved its photostability to the UVB radiation. Moreover, acceptable, biocompatible and accessible materials for topical use, such as, ethanol, decaethylene glycol mono-dodecyl ether, water and oleic acid, composed the system.

On the other hand, the chemometric analysis allowed to corroborate the photolysis mechanisms of the OMC, which include a photoisomerization step and the generation of by-products. Besides, kinetic rate constants corresponding to the photoisomerization of the OMC were obtained.

With respect to its efficiency as sunscreen, the proposed OMC-ME presents a satisfactory SPF, increasing almost eight times the amount of time to produce an erythema on the skin; that is to say, before beginning to burn a person exposed to a low level of UVB radiation.

Acknowledgments

The authors gratefully acknowledge the financial support of Consejo Nacional de Investigaciones Científicas y Técnicas (PIP 11220120100625) and Universidad Nacional del Sur (PGI 24Q054).

References

[1] C. Cole, Sunscreen Formulation: Optimizing Efficacy of UVB and UVA Protection, Principles and Practice of Photoprotection, Springer, Switzerland 2016, pp. 275–287.
[2] N. Serpone, D. Dondi, A. Albini, Inorganic and organic UV filters: their role and efficacy in sunscreens and suncare products, Inorg. Chim. Acta 360 (2007) 794–802.
[3] E. Damiani, P. Astolfi, J. Giesinger, T. Ehlis, B. Herzog, L. Greci, W. Baschong, Assessment of the photodegradation of UV-filters and radical-induced peroxidation in cosmetic sunscreen formulations, Free Radic. Res. 44 (3) (2010) 304–312.
[4] J. Kockler, M. Oelgemöller, S. Robertson, B.D. Glass, Photostability of sunscreens, J. Photoch. Photobio. C 13 (2012) 91–110.
[5] L.A. Mac Manus-, M.L. Spencer, J.L. Tse, A.E. Klein, Kracunas, aqueous photolysis of the organic ultraviolet filter chemical octyl methoxycinnamate, Environ. Sci. Technol. 45 (2011) 3931–3937.
[6] B.I. Olvera-Martínez, J. Cázares-Delgadillo, S.B. Calderilla-Fajardo, R. Villalobos-García, A. Ganem-Quintanar, D. Quintanar-Guerrero, Preparation of polymeric nanocapsules containing octyl methoxycinnamate by the emulsification-diffusion technique: penetration across the stratum corneum, J. Pharm. Sci. 94 (2005) 1552–1559.
[7] C. Puglia, F. Bonina, L. Rizza, P. Blasi, A. Schoubben, R. Perrotta, M. Stella Tarico, E. Damiani, Lipid nanoparticles as carrier for octyl methoxycinnamate: *In vitro* percutaneous absorption and photostability studies, J. Pharm. Sci. 101 (2012) 301–311.
[8] M.E. Carlottia, S. Sapino, D. Vione, C. Minero, M. Trotta, M. Gallarate, Photostability of octyl p-methoxycinnamate in o/w emulsions and in SLNs vehicled in the emulsions, J. Disper. Sci. Technol. 28 (2007) 1034–1043.
[9] D.P. Acharya, P.G. Hartley, Progress in microemulsion characterization, Curr. Opin. Colloid Interface Sci. 17 (2012) 274–280.
[10] F.H. Xavier-Junior, C. Vauthier, A.R.V. Morais, E.N. Alencar, E.S.T. Egito, Microemulsion Systems Containing Bioactive Natural Oils: An Overview on the State of the Art, Drug Dev. Ind, Pharm, 2016https://doi.org/10.1080/03639045.2016.1235186.
[11] A. de Juan, R. Tauler, Chapter 2 - multivariate curve resolution-alternating least squares for spectroscopic data, Data Handl Sci Techn. 30 (2016) 5–51.
[12] C. Ruckebusch, L. Blanchet, Multivariate curve resolution: a review of advanced and tailored applications and challenges, Anal. Chim. Acta 765 (2013) 28–36.
[13] M. Razuc, M. Garrido, Y.S. Caro, C.M. Teglia, H.C. Goicoechea, B.S. Fernández Band, Hybrid hard- and soft-modelling of spectrophotometric data for monitoring of ciprofloxacin and its main photodegradation products at different pH values, Spectrochim. Acta Mol. Biomol. Spectrosc. 106 (2013) 146–154.
[14] A. de Juan, M. Maeder, M. Martinez, R. Tauler, Combining hard- and soft-modelling to solve kinetic problems, Chem. Intell. Lab, Syst. 54 (2000) 123–141.
[15] R. Jansen, U. Osterwalder, S.Q. Wang, M. Burnett, H.W. Lim, Photoprotection: part II. Sunscreen: development, efficacy, and controversies, J. Am. Acad. Dermatol. 69 (2013) 867.e1–867.e14.
[16] Multivariate Curve Resolution Homepage, http://www.mcrals.info.
[17] MATLAB®, TheMathworks, Inc., Natick, MA, USA.
[18] J.S. Mansur, M.N.R. Breder, M.C.A. Mansur, R.D. Azulay, Determination of sun protection factor by spectrophotometry, An. Bras. Dermatol. 61 (1986) 121–124.
[19] R.M. Sayre, P.P. Agin, G.J. Levee, E. Marlowe, A comparison of *in vivo* and *in vitro* testing of sunscreening formulas, Photochem. Photobiol. 29 (1979) 559–566.
[20] K.M. Hanson, S. Narayanan, V.M. Nichols, C.J. Bardeen, Photochemical degradation of the UV filter octyl methoxycinnamate in solution and in aggregates, Photochem. Photobiol. Sci. 14 (2015) 1607–1616.
[21] X.P. Chang, C.X. Li, B.B. Xie, G. Cui, Photoprotection mechanism of *p*-methoxy methylcinnamate: a CASPT2 study, J. Phys. Chem. A 119 (2015) 11488–11497.
[22] R. Wolf, D. Wolf, P. Morganti, V. Ruocco, Sunscreens, Clinic. Dermatol. 19 (2001) 452–459.
[23] E.A. Dutra, D.A.G.C. Oliveira, E.R.M.K. Hackmann, M.I.R.M. Santoro, Determination of sun protection factor (SPF) of sunscreens by ultraviolet spectrophotometry. Braz, J. Pharm. Sci. 40 (2004) 381–385.
[24] V. Trotta, F. Goios, H. Monteiro, I.F. Almeida, S. Scalia, Influence of lipid microparticle encapsulation on *in vitro* efficacy, photostability and water resistance of the sunscreen agents, octyl methoxycinnamate and butyl methoxydibenzoylmethane, Drug Dev. Ind. Pharm. 40 (2014) 1233–1239.